Measurement of the optical path length difference in an interferometer using a sinusoidally frequency-modulated light source

Shumpei Shimada,[1] **Makoto Shizuka,**[1] **Neisei Hayashi,**[2] **Yosuke Mizuno,**[1,*] **and Kentaro Nakamura**[1]

[1]*Laboratory for Future Interdisciplinary Research of Science and Technology, Tokyo Institute of Technology, 4259, Nagatsuta-cho, Midori-ku, Yokohama 226-8503, Japan*
[2]*Research Center for Advanced Science and Technology, The University of Tokyo, 4-6-1, Komaba, Meguro-ku, Tokyo 153-8904, Japan*
Corresponding author: ymizuno@sonic.pi.titech.ac.jp

We develop a technique for measuring the optical path length difference (OPLD) in an interferometer using a frequency-modulated light source. Compared with conventional methods, this technique offers a high sampling rate, high precision, and cost efficiency, and is capable of determining which of the two optical paths is longer. In addition, we show that this technique works properly even when the OPLD is significantly longer than the coherence length of the light source. © 2016 Optical Society of America

1. INTRODUCTION

For the past several decades, fundamental sensing techniques based on fiber-optic interferometry have been studied in order to measure a variety of physical parameters, such as reflectivity, loss, strain, temperature, displacement, vibration, pressure, humidity, profile, refractive index, concentration, pH, and rotation [1–6]. Some of the fiber-optic interferometers used in such measurements are composed of two light paths: a signal path, which contains an optical circulator, and a reference path. The optical path length difference (OPLD) between these two paths generally plays a significant role in the operation of the system. For instance, let's consider using a technique known as optical correlation-domain reflectometry (OCDR) [7–16] in conjunction with a distributed reflectivity sensing system. If the zero-OPLD point is located in the fiber under test (FUT; i.e., the second port of the circulator), in theory the measurement cannot be performed. Another example is a technique known as Brillouin OCDR [17–19] in conjunction with a distributed strain and temperature sensing system. Even when the zero-OPLD point is located outside the FUT, unless the OPLD is carefully selected, the signal-to-noise ratio (SNR) of the measurement drastically deteriorates because of the overlap of the interference pattern on the Brillouin gain spectrum [19]. Thus, it is of crucial importance to measure and control the OPLD in an interferometer that includes an optical circulator.

Direct measurement of the OPLD is, however, sometimes difficult, because general interferometers contain various optical devices with unknown fiber lengths, such as optical amplifiers,

external modulators, and kilometer-order delay lines. Therefore, several techniques for measuring the OPLD indirectly have been developed. One such technique works by exploiting the interval between the interference fringes observed using a spectrum analyzer [19–22]. This method is simple, though it does not allow us to judge which of the two paths is longer; furthermore, the visibility of the interference pattern becomes extremely low when the OPLD is significantly longer than the coherence length of the light source (or when the frequency resolution of the spectrum analyzer is not sufficiently high). Another method is based on the so-called time-of-flight technique [23–25], wherein optical pulses are simultaneously injected into the two paths, and the delay between the reflected pulses is subsequently measured. However, preparing such optical pulses can be costly, and this method does not provide any information concerning which of the paths is longer. In addition, numerous reflected pulses are generally utilized in order to improve the SNR, resulting in a relatively long measurement time (for instance, up to several minutes).

In order to mitigate the aforementioned drawbacks of the conventional techniques, in this work we develop an OPLD measurement technique for an interferometer that contains an optical circulator. By using a frequency-modulated light source, our technique can achieve a high sampling rate (corresponding to a short measurement time of ~10 ms), high precision, and cost efficiency. Moreover, we demonstrate that this technique can determine which of the two optical paths is longer, and that the OPLD can be correctly obtained even when it is significantly longer than the laser coherence length.

2. PRINCIPLE

The basic configuration of a fiber-optic interferometer that contains an optical circulator is schematically illustrated in Fig. 1, where an FUT is connected to the second port of the circulator. In order to calculate the OPLD between the signal and reference paths, here we exploit one of the useful techniques for distributed reflectivity measurements—namely, OCDR [9–16]—by using a synthesized optical coherence function (SOCF) [14]. This system operates based on optical correlation control by the frequency modulation of laser output. The methods involved in frequency modulation can be classified into two categories: sinusoidal modulation [9–11] and stepwise modulation [12–14], which includes the use of optical frequency combs [15,16]; the former method is reported to be more cost efficient [9–11].

In a standard SOCF-OCDR system based on sinusoidal modulation [9–11], optical heterodyne detection using an acousto-optic modulator (AOM) is performed in order to shift the Fresnel spectrum by several tens of megahertz, thereby avoiding the overlap of low-frequency noise from the electrical devices. However, we have recently succeeded in excluding the optical heterodyne detection from the measurement process (i.e., eliminating the need for an AOM) by exploiting the foot of the Fresnel spectrum [26]. This results in electrical signal processing in the frequency range near dc (up to several megahertz) and, furthermore, reduces the cost of the relevant devices. High-speed operation has also been demonstrated by tracking a moving reflection point.

In an SOCF-OCDR system (with or without the use of an AOM), the optical frequency of the laser output is sinusoidally modulated at f_m, thereby generating periodical correlation peaks along an FUT [14]. The measurement range d_m is determined by the interval between the correlation peaks, which is inversely proportional to f_m as follows:

$$D = \frac{c}{2nf_m}, \tag{1}$$

where c is the velocity of light in a vacuum and n is the refractive index of the fiber core. By sweeping f_m, the correlation peak, which can be regarded as the sensing position, can be scanned along the FUT in order to acquire the reflectivity distribution. The spatial resolution of the system is given by [27]

$$\Delta z \cong \frac{0.76c}{\pi n \Delta f}, \tag{2}$$

where Δf is the modulation amplitude of the optical frequency.
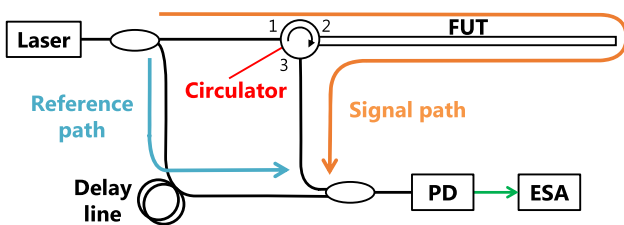
Here, we develop a new method of calculating the OPLD between the signal and reference paths by using the operating principle of SOCF-OCDR. The zeroth-order correlation peak is always located at a zero-OPLD point, the location of which is fixed regardless of the modulation frequency f_m (Fig. 2). When the neighboring first-order correlation peak is located at the FUT end, where optical reflectivity is high due to Fresnel reflection, the OPLD can be calculated as the product of the core's refractive index n and twice the correlation peak interval [i.e., the measurement range d_m given by Eq. (1)]. In general, when neighboring correlation peaks are located at the FUT end, the difference in their f_m values (denoted by Δf_m) is the same as the f_m value when the first-order correlation peak is located at the FUT end, irrespective of their peak orders. Therefore, by acquiring the reflectivity (or reflection power) as a function of f_m and obtaining Δf_m from an arbitrary set of two neighboring reflectivity peaks (corresponding to Fresnel reflection at the FUT end), the OPLD can be calculated as follows:

$$OPLD = \frac{c}{\Delta f_m}. \tag{3}$$

3. EXPERIMENTAL SETUP

Figure 3 depicts the experimental setup, which represents an AOM-free SOCF-OCDR system. It contains an optical circulator in the signal path; moreover, several dummy devices are employed in order to demonstrate that this method is applicable to complicated interferometers. A laser diode with a wavelength of 1550 nm and a linewidth of ~1 MHz (and thus a coherence length of ~200 m) was used as a light source. The driving current of the laser was directly modulated with a bias of 80 mA. The laser output was amplified to 18 dBm using an erbium-doped fiber amplifier (EDFA) and was injected into the FUT. Both the reflected light and the reference light were also amplified to 3 dBm using EDFAs. Polarization controllers (PCs), which were used to adjust the polarization states, were inserted in both optical paths. Various lengths of delay lines were inserted in each path in order to adjust the OPLD. The modulation amplitude Δf was fixed at 0.75 GHz, which corresponds to a nominal spatial resolution of 66 mm [see Eq. (2)]. For AOM-free operation, a 2 MHz component of the Fresnel reflection spectrum [output of a photodiode (PD)] observed using an electrical spectrum analyzer (ESA) was selectively acquired with an oscilloscope (OSC) in order to maximize the SNR [26]. The resolution bandwidth (RBW) and
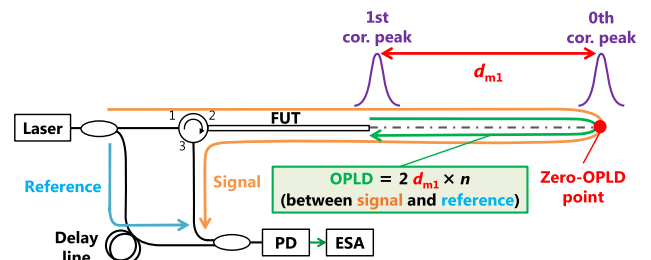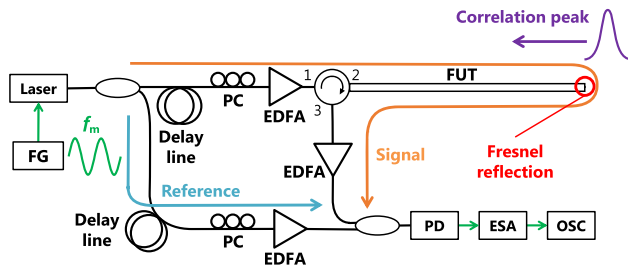

Fig. 1. Basic configuration of a fiber-optic interferometer that contains an optical circulator in the signal path. ESA, electrical spectrum analyzer; FUT, fiber under test; PD, photodiode.

Fig. 2. Calculation principle of the optical path length difference (OPLD).

Fig. 3. Schematic setup for experimental demonstration. EDFA, erbium-doped fiber amplifier; FG, function generator; OSC, oscilloscope; PC, polarization controller.

video bandwidth (VBW) of the ESA were set to 300 and 1 kHz, respectively. Data averaging was performed 100 times on the OSC (unless otherwise stated) in order to secure a high SNR, corresponding to a total measurement time of ∼1 s (10 ms for one sampling).

4. EXPERIMENTAL RESULTS

The first demonstration was performed for a signal path that was shorter than the reference path by ∼50 m. Figure 4(a) shows the reflection power dependence on the modulation frequency f_m in the range from 3 to 15 MHz. Two sets of peaks, each of which consisted of one small and one large peak, were observed. Using the large peaks corresponding to the Fresnel reflection at the FUT end, the frequency difference Δf_m was calculated to be 6.142 MHz, which agrees with the f_m value of the large peak at the lower frequency. This is because the set of peaks at the lower frequency corresponds to the first-order correlation peak. By substituting the Δf_m value into Eq. (3), the OPLD was calculated to be 48.84 m. (The validity of this value is discussed below.)

The smaller peaks correspond to the reflection from the circulator. In general, when the signal path is shorter than the reference path, as f_m increases, the correlation peaks move from proximal (circulator) to distal (FUT end) positions, resulting in the appearance of the small peak followed by the appearance of the large peak. In contrast, when the signal path is longer than the reference path, as f_m increases, the correlation peaks move from distal to proximal positions, resulting in the
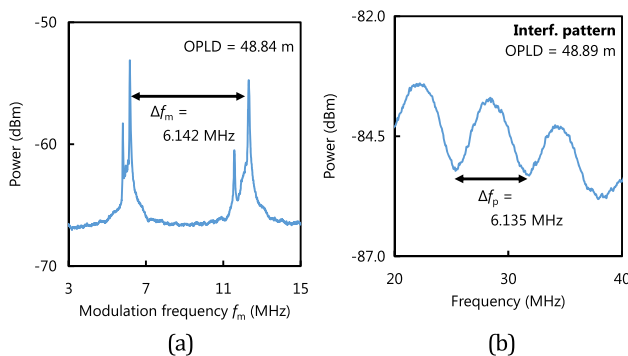
appearance of the large peak followed by the appearance of the small peak. Thus, using the order in which the small and large peaks appear within each set of peaks, we can ascertain which of the two paths is longer; this logical procedure is (to our knowledge) unique to our method.

The calculated value of the OPLD (48.84 m) was then validated by measuring the same OPLD using a standard technique based on an interference pattern, which is shown in Fig. 4(b). The RBW and VBW of the ESA were set to 10 and 0.1 kHz, respectively. The average period of the interference pattern Δf_p (calculated using multiple peaks/dips) was 6.135 MHz; this corresponds to an OPLD of 48.89 m ($= c/\Delta f_p$), thereby indicating impressive agreement between the two methods. Because the widths of the peaks in Fig. 4(a) are narrower than those in Fig. 4(b), the OCDR-based method provides higher precision when a simple fringe-counting technique is used.

Subsequently, the same measurements were performed for a signal path that was longer than the reference path by ∼50 m. Figure 5(a) shows the reflection power dependence on f_m. The frequency difference Δf_m was 5.666 MHz, which corresponds to an OPLD of 52.95 m; this was verified by the interference pattern in Fig. 5(b) with a Δf_p value of 5.680 MHz, which corresponds to an OPLD of 52.82 m. As f_m increases, the large peak appears first and is followed by the small peak. This order is opposite to that in Fig. 4(a), which indicates that the signal path is longer than the reference path in this case.

We also measured the OPLD for a signal path that was shorter than the reference path by ∼1 km, which is longer than the coherence length of the laser (∼200 m). From the reflection power dependence on f_m [Fig. 6(a)], Δf_m was calculated to be 210 kHz, which corresponds to an OPLD of 977 m. From the interference pattern [Fig. 6(b)], Δf_p was evaluated to be 211 kHz, which corresponds to an OPLD of 974 m. However, the visibility of the pattern was so low that precise measurement was relatively difficult.
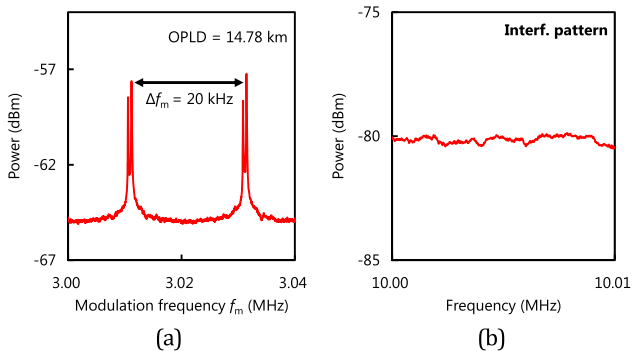
Additionally, we performed the same measurements for a signal path that was shorter than the reference path by ∼15 km, which is significantly longer than the laser coherence length. The reflection power dependence on f_m was obtained [Fig. 7(a)], and Δf_m was calculated to be 20 kHz, which corresponds to an OPLD of 14.78 km. However, the interference

Fig. 4. (a) Reflection power dependence on the modulation frequency f_m, (b) interference pattern measured for a signal path that is shorter than the reference path by ∼50 m.
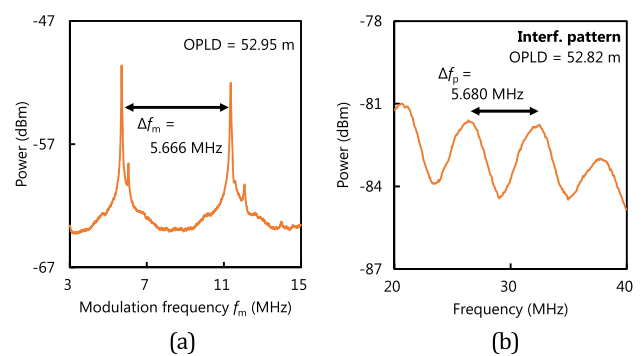
Fig. 5. (a) Reflection power dependence on the modulation frequency f_m, (b) interference pattern measured for a signal path that is longer than the reference path by ∼50 m.
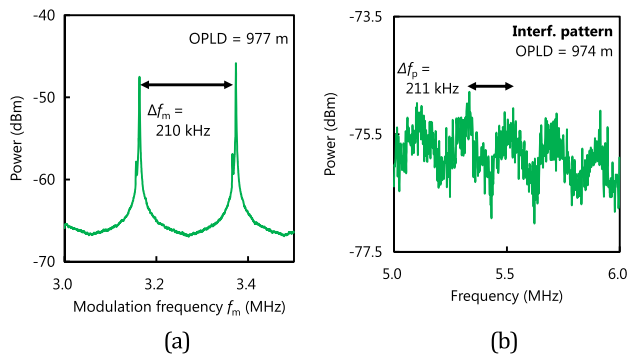
Fig. 6. (a) Reflection power dependence on the modulation frequency f_m, (b) interference pattern measured for a signal path that is shorter than the reference path by ∼1 km.
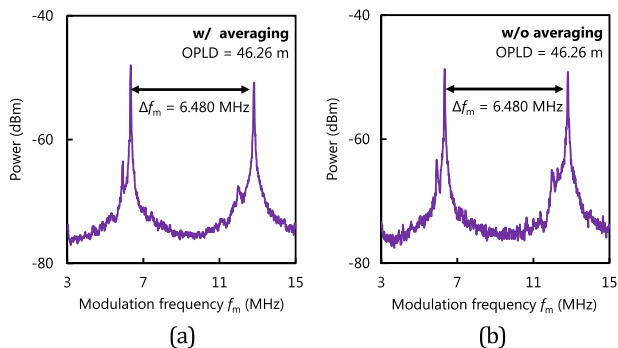

Fig. 7. (a) Reflection power dependence on the modulation frequency f_m, (b) interference pattern measured for a signal path that is shorter than the reference path by ∼15 km.

pattern was not observed, as shown in Fig. 7(b). The ability to measure an OPLD that is significantly longer than the coherence length of the laser is one of the important advantages of this method. (It is worth noting that SOCF-OCDR has been shown to possess a measurement range much longer than the laser coherence length [28].)

Finally, the averaging effect was evaluated using the data obtained for a signal path that was shorter than the reference

Fig. 8. Reflection power dependencies on the modulation frequency f_m (a) with and (b) without averaging (100 times), measured for a signal path that is shorter than the reference path by ∼50 m.

path by ∼50 m. Figures 8(a) and 8(b) show the reflection power dependencies on f_m with and without averaging (100 times). Even without averaging (leading to a measurement time of 10 ms), the OPLD was correctly calculated to be 46.26 m. High-speed measurability is also one of the advantages of this method, as compared with other techniques that exploit interference patterns or optical pulses.

5. CONCLUSION

Based on the principle of the AOM-free SOCF-OCDR, a technique for measuring the OPLD in an interferometer was developed. We demonstrated its high-speed operation, high precision, and, most importantly, its capability of determining which of the two optical paths is longer. We also experimentally demonstrated that this technique works properly even when the OPLD is significantly longer than the laser coherence length. We believe that this technique will serve as a promising candidate for implementing OPLD measurement systems in future studies.

REFERENCES

1. Y. J. Rao and D. A. Jackson, "Principles of fiber-optic interferometry," in *Optical Fiber Sensor Technology*, K. T. V. Grattan and B. T. Meggitt, eds. (Springer, 2000), pp. 167–191.
2. A. D. Drake and D. C. Leiner, "Fiber-optic interferometer for remote subangstrom vibration measurement," Rev. Sci. Instrum. **55**, 162–165 (1984).
3. C. E. Lee and H. F. Taylor, "Fiber-optic Fabry-Perot temperature sensor using a low- coherence light source," J. Lightwave Technol. **9**, 129–134 (1991).
4. D. P. Hand, T. A. Carolan, J. S. Barton, and J. D. C. Jones, "Profile measurement of optically rough surfaces by fiber-optic interferometry," Opt. Lett. **18**, 1361–1363 (1993).
5. L. Yuan, "White-light interferometric fiber- optic strain sensor from three-peak- wavelength broadband LED source," Appl. Opt. **36**, 6246–6250 (1997).
6. T. K. Yadav, R. Narayanaswamy, M. H. Abu Bakar, Y. M. Kamil, and M. A. Mahdi, "Single mode tapered fiber-optic interferometer based refractive index sensor and its application to protein sensing," Opt. Express **22**, 22802–22807 (2014).
7. R. C. Youngquist, S. Carr, and D. E. N. Davies, "Optical coherence-domain reflectometry: a new optical evaluation technique," Opt. Lett. **12**, 158–160 (1987).
8. E. A. Swanson, D. Huang, M. R. Hee, J. G. Fujimoto, C. P. Lin, and C. A. Puliafito, "High-speed optical coherence domain reflectometry," Opt. Lett. **17**, 151–153 (1992).
9. K. Hotate, M. Enyama, S. Yamashita, and Y. Nasu, "A multiplexing technique for fibre Bragg grating sensors with the same reflection wavelength by the synthesis of optical coherence function," Meas. Sci. Technol. **15**, 148–153 (2004).
10. Z. He, T. Tomizawa, and K. Hotate, "High-speed high-reflectance-resolution reflectometry by synthesis of optical coherence function," IEICE Electron. Express **3**, 122–128 (2006).
11. Z. He, M. Konishi, and K. Hotate, "A high-speed sinusoidally frequency-modulated optical reflectometry with continuous modulation-frequency sweeping," Proc. SPIE **7004**, 70044L (2008).
12. K. Hotate and O. Kamatani, "Reflectometry by means of optical-coherence modulation," Electron. Lett. **25**, 1503–1505 (1989).
13. Z. He and K. Hotate, "Distributed fiber-optic stress-location measurement by arbitrary shaping of optical coherence function," J. Lightwave Technol. **20**, 1715–1723 (2002).

14. K. Hotate, "Application of synthesized coherence function to distributed optical sensing," Meas. Sci. Technol. **13**, 1746–1755 (2002).

15. Z. He, H. Takahashi, and K. Hotate, "Optical coherence-domain reflectometry by use of optical frequency comb," in *Conference on Lasers and Electro-Optics* (2010), paper CFH4.

16. H. Takahashi, Z. He, and K. Hotate, "Optical coherence domain reflectometry by use of optical frequency comb with arbitrary-waveform phase modulation," in *European Conference on Optical Communication* (2010), paper Tu.3.F.4.

17. Y. Mizuno, W. Zou, Z. He, and K. Hotate, "Proposal of Brillouin optical correlation-domain reflectometry (BOCDR)," Opt. Express **16**, 12148–12153 (2008).

18. Y. Mizuno, W. Zou, Z. He, and K. Hotate, "Operation of Brillouin optical correlation-domain reflectometry: theoretical analysis and experimental validation," J. Lightwave Technol. **28**, 3300–3306 (2010).

19. Y. Mizuno, N. Hayashi, and K. Nakamura, "Fiber-optic interferometry using narrowband light source and electrical spectrum analyzer: influence on Brillouin measurement," J. Lightwave Technol. **32**, 4734–4740 (2014).

20. L. V. Ngyuen, D. Hwang, S. Moon, D. S. Moon, and Y. Chung, "High temperature fiber sensor with high sensitivity based on core diameter mismatch," Opt. Express **16**, 11369–11375 (2008).

21. A. A. Jasim, N. Hayashi, S. W. Harun, H. Ahmad, R. Penny, Y. Mizuno, and K. Nakamura, "Refractive index and strain sensing using inline Mach-Zehnder interferometer comprising perfluorinated graded-index plastic optical fiber," Sens. Actuators A **219**, 94–99 (2014).

22. K. S. Park, H. Y. Choi, S. J. Park, U. C. Paek, and B. H. Lee, "Temperature robust refractive index sensor based on a photonic crystal fiber interferometer," IEEE Sens. J. **10**, 1147–1148 (2010).

23. K. Aoyama, K. Nakagawa, and T. Itoh, "Optical time domain reflectometry in a single-mode fiber," IEEE J. Quantum Electron. **17**, 862–868 (1981).

24. S. V. Shatalin, V. N. Treschikov, and A. J. Rogers, "Interferometric optical time-domain reflectometry for distributed optical-fiber sensing," Appl. Opt. **37**, 5600–5604 (1998).

25. T. Kurashima, T. Horiguchi, H. Izumita, S. Furukawa, and Y. Koyamada, "Brillouin optical-fiber time domain reflectometry," IEICE Trans. Commun. **76**, 382–390 (1993).

26. M. Shizuka, S. Shimada, N. Hayashi, Y. Mizuno, and K. Nakamura, "Optical correlation-domain reflectometry without optical frequency shifter," Appl. Phys. Express **9**, 032702 (2016).

27. K. Hotate and K. Kajiwara, "Proposal and experimental verification of Bragg wavelength distribution measurement within a long-length FBG by synthesis of optical coherence function," Opt. Express **16**, 7881–7887 (2008).

28. M. Kashiwagi and K. Hotate, "Long range and high resolution reflectometry by synthesis of optical coherence function at region beyond the coherence length," IEICE Electron. Express **6**, 497–503 (2009).